SMiRT–12 / K. Kussmaul (Editor)

J01/6

DYNAMIC ANALYSIS OF A PWR MAIN STEAM LINE FOLLOWING POSTULATED PIPE RUPTURES

M.C. Smith

Nuclear Electric plc, Berkeley Technology Centre, Berkeley, Gloucestershire GL13 9PB, England

ABSTRACT

Transient dynamic analyses of pipe breaks within the main steam system of the Sizewell 'B' power station were performed to generate internal forces and moments for use in fracture mechanics analyses. The analyses included a number of sensitivity studies to identify the most important modelling and analysis variables.

1. INTRODUCTION

In the Sizewell 'B' PWR the sections of the main steam lines containing the safety relief valves (SRV's) and main steam isolation valves (MSIV's) are of particular importance to plant safety. All four steam lines are adjacent to one another, and it is necessary to show that cascade failure of multiple steam lines is not possible. The safety case for this pipework thus includes a fracture mechanics assessment. This demonstrates that under extreme fault condition loading the system is tolerant to much larger defects than those expected to be present at the end of plant life. Amongst the most important loading conditions are the dynamic loads due to pipe breaks downstream of the SRV's and MSIV.

The relevant sections of the steam lines are contained in a separate steam and feed cell between primary containment upstream and the mechanical annex and turbine hall downstream. Four lines pass through the cell in parallel, and each includes five SRV's, a branch to a power operated relief valve (PORV), and an MSIV. The steam and feed cell pipework is fully isolated from that in containment. It is also isolated from that downstream by a torsional restraint system in each line which allows axial float while restricting radial movement and rotation of the steam line. This is designed to isolate the steam and feed cell from the effects of downstream pipe breaks, and consists of a thickened pipe section within close-fitting embedments. Downstream of the torsional restraint all four lines are joined by a cross-under pipe before passing round vertical thermal expansion loops to the turbine headers.

Pipe break loads were calculated by performing non-linear large-displacement transient dynamic analyses of a number of possible pipe breaks using the ABAQUS finite element code (Ref. 1). The main steam line is a relatively complex system, and it is not possible to predict in advance what combination of modelling variables will predict the most appropriate loads on the components of interest. Thus the dynamic analysis included a number of sensitivity studies to identify the most important modelling assumptions.

The forces and moments generated by these analyses were used in fracture assessments of critical components in the steam and feed cell.

2. MATHEMATICAL MODELLING

Five models of the main steam line were used to cover the whole range of analyses required:

1. A simple planar model of one steam line, beginning at the containment penetration and ending at break location C (see Figs 1 and 2 for break locations). All the valves were represented by rigid

beams and offset masses, and no branch pipework in the steam and feed cell was modelled. The cross-under pipe in the mechanical annex was also omitted. This model was used to examine the effect of torsional restraint gap configuration and blowdown force magnitude on the response of the system to break C.

2. A much more complete model of the pipework within the steam and feed cell, including a detailed representation of the PORV branch pipework and a more representative MSIV model, also ending at break C. This model was used to examine the effects of modelling refinement on the response of the system to break C.
3. Model 2 extended to break D. This model was used to examine the response of the system to break D, and is shown in Fig 1.
4. Model 2 extended to break E by including a section of the cross-under pipe. This model was used to examine the response of the system to break E.
5. Model 4 extended to include the full cross-under pipe and sections of all four steam lines downstream of the torsional restraint. This model was used to examine the effect of including additional load paths to react the blowdown force, and is shown in Fig 2.

The models were constructed using ELBOW32, PIPE32 and B32 Timoshenko beam elements. ELBOW32 elements allow pipe ovalisation and warping, and were used for all bends and for pipework downstream of the torsional restraint which may yield or collapse. PIPE32 elements were used for all other plain pipework and nozzles. B32 elements were used for complex sections in the MSIV and torsional restraint. Spring hangers and foundation flexibility's were represented using SPRING1 elements. Note that all spring hangers and supports in the mechanical annex were omitted from the models. The bodies of smaller valves were modelled as rigid beams using multi-point constraints. Valve and flange masses were added using MASS elements.

The gaps in the torsional restraint system were expected to have a large effect on the response upstream. Simple gap elements were found to cause convergence problems, so the gaps were modelled as non-linear springs with a very low initial stiffness and a rapid rise to the foundation stiffness at the point of closure. The torsional restraint system consists of a pipe forging with two greatly thickened sections, and two restraint structures . The upstream, torsional restraint restrains radial motion and rotation about the pipe axis of the main steam line, while the downstream, radial restraint restrains only radial motion. The rotational and radial clearances in the upstream restraint are coupled, with rotation reducing the radial clearance. The gap size and initial pipe position in both restraints are also functions of system temperature and loading condition. This complex geometry was modelled using simple uncoupled vertical, lateral, and rotational springs. At operating temperature the nominal radial gap in both torsional and radial restraints is ± 2.8 mm. The rotational clearance at the torsional restraint for a centrally positioned pipe is $\pm 0.40^{\circ}$.

The materials of the system were represented using piece-wise linear stress-strain curves based on best-estimate material properties. This property basis allows realistic predictions of the forces transmitted through any plastic hinges formed in the whipping pipe.

The system blowdown force transient was assumed to be a linear rise over 5 ms to a constant peak value of 2.6 MN. The transient was applied using nodal follower forces at the pipe bends in the mechanical annex.

The analysis matrix is shown in Table 1. The following variables were examined:

- The effect of break location and the direction of the blowdown force. Three break locations were chosen for analysis, and these are labelled C, D and E in Figs 1 and 2.
- The gap size and initial pipe position in the torsional restraint. Four initial gap sizes and three initial pipe positions were examined for break C, and three gap configurations for break E.
- The complexity of modelling required within the steam and feed cell. Both the extent of branch pipe modelling and the refinement of MSIV modelling were considered, for break C.

- The extent of modelling within the mechanical annex and turbine hall. All four steam lines are connected within the mechanical annex, so a single pipe break has multiple load paths to ground. The pessimism involved in neglecting these additional load paths was evaluated for break C.
- The effect of simultaneous release of equilibrium internal loads in the pipe and application of the blowdown force at the pipe break. This was examined for break C.

3. RESULTS

The pipe downstream of the torsional restraint suffers an uncontrolled whip for all three break locations, and a plastic hinge forms at the downstream end of the torsional restraint (breaks C and E) or at the first bend in the mechanical annex (break D). Pipe collapse at the plastic hinge occurs at around 120 ms for breaks C and E, and somewhat earlier for break D. Peak loads on the downstream end of the torsional restraint are insensitive to the gap configuration, and are determined by the collapse moment of the pipework and the direction of the pipe whip. The analysis using Model 5 showed that the inclusion of additional load paths in the mechanical annex slows the velocity of the pipe whip somewhat, but is not sufficient to prevent the development of a plastic hinge, and therefore does not significantly reduce the peak load on the torsional restraint.

The pipework in the steam and feed cell suffers an oscillatory transient elastic response, driven initially by an elastic deformation wave propagating through the open gaps in the torsional restraint, and later by rigid body motion of the torsional restraint forging until the gaps close. The response occurs in the main elastic modes of the system, and only modes below about 50 Hz are excited. The initial loading transient for the steam and feed cell is very short in duration. Once the torsional restraint gaps close, events in the annex do not affect the steam and feed cell pipework. Thus, for example, in break C the gaps close at ~25 ms, at which time the loading transient on the steam and feed cell is effectively over. If the gaps re-open later in the transient, then the steam and feed cell will be loaded again. This occurs for break D, and results in the highest bending moments on the main steam line in the steam and feed cell.

The results showed that the size and configuration of the gaps in the torsional restraint were the most important variables governing the response of the steam and feed cell components. These are loaded impulsively by two events: an initial elastic transverse half-wave propagating along the steam line from the break, and later gross motion of the torsional restraint within its supports. Both these events are very sensitive to the initial gap configuration, see Fig 3.

- The initial deformation wave is attenuated if the gap size is smaller than the wave amplitude, and is unchanged at greater gap sizes. The oscillatory response of the system upstream of the MSIV is controlled by this initial deformation pulse, so it saturates beyond a certain gap size. Because only a half-wave is generated, only the gap on one side of the pipe is important. Thus the two non-symmetric gap analyses produced very different responses to this event, despite the total diametric gap being constant. The worst condition is slightly unexpected, since a +y-direction blowdown force produces a -y direction deformation pulse. The worst gap condition is thus to start with the +y gaps closed.
- Gross motion of the torsional restraint within its supports obviously increases with the diametric gap size. However, the initial gap offset is also important, since it determines the severity of the final closure event at the upstream gaps. Again, it is more severe to start with the +y gaps closed.

The torsional restraint thus succeeds in its primary design objective of preventing plastic hinge formation within the no-break zone. However, the clearances within it are very important in determining the elastic transient loads developed upstream.

The analysis which released the internal forces in the pipe at the same time as applying the blowdown forces showed that it is pessimistic to cover the effect of releasing these forces by simple static combination of the peak forces and moments due to normal operation of the steam line with those from a pipe break analysis using only the blowdown force transient.

4. FRACTURE ASSESSMENTS

Appropriate forces and moments on critical components within the steam and feed cell were then combined with those due to other coincident loading events, obtained from standard quasi-static and response spectrum pipework analyses. These combined loads were applied to detailed local FE models of the MSIV, and the SRV and PORV headers, and peak stresses within the pressure boundary evaluated. Limiting flaw size assessments were performed using the R6 method (Ref. 2). These demonstrated adequate margin over the maximum possible pre-existing flaw size.

5. REFERENCES

1. ABAQUS User's Manual, version 4.8, Hibbett Karlsson and Sorenson Inc, Providence, Rhode Island, 1989.
2. "R6: Assessment of the integrity of structures containing defects", report R/H/R6 rev 3, Nuclear Electric, reprinted February 1988 with amendments up to May 1991.

6. TABLES AND FIGURES

Table 1. Analysis matrix

Model used	Break location	Break force	Gap configuration
1	C	2.6 MN blowdown	no gaps
1	C	2.97 MN blowdown	no gaps
1	C	2.6 MN blowdown	+/-1.4 mm (vertical only)
1	C	2.6 MN blowdown	+/-2.8 mm (vertical only)
1	C	2.6 MN blowdown	+/-4.2 mm (vertical only)
1	C	2.6 MN blowdown	+5.6 -0.0 mm (vertical only)
1	C	2.6 MN blowdown	+0 -5.6 mm (vertical only)
2	C	2.6 MN blowdown	+/-2.8 mm (vertical and lateral) free rotation
2	C	2.6 MN blowdown plus release of normal operation thermal loads	+/-2.8 mm (vertical and lateral) free rotation
3	D	2.6 MN blowdown	+/-2.8 mm (vertical and lateral) +/-0.32^{o} (rotational)
4	E	2.6 MN blowdown	+/-2.8 mm (vertical and lateral) +/-0.32^{o} (rotational)
4	E	2.6 MN blowdown	+/-2.8 mm (vertical and lateral) at downstream restraint). 0.0 mm (vertical and lateral) and +/-0.32^{o} (rotational) at upstream restraint).
4	E	2.6 MN blowdown	+/-2.8 mm (vertical and lateral) at downstream restraint). 0.0 mm (vertical and lateral) and +/-0.40^{o} (rotational) at upstream restraint).
5	C	2.6 MN blowdown	+/-2.8 mm (vertical and lateral) +/-0.32^{o} (rotational)

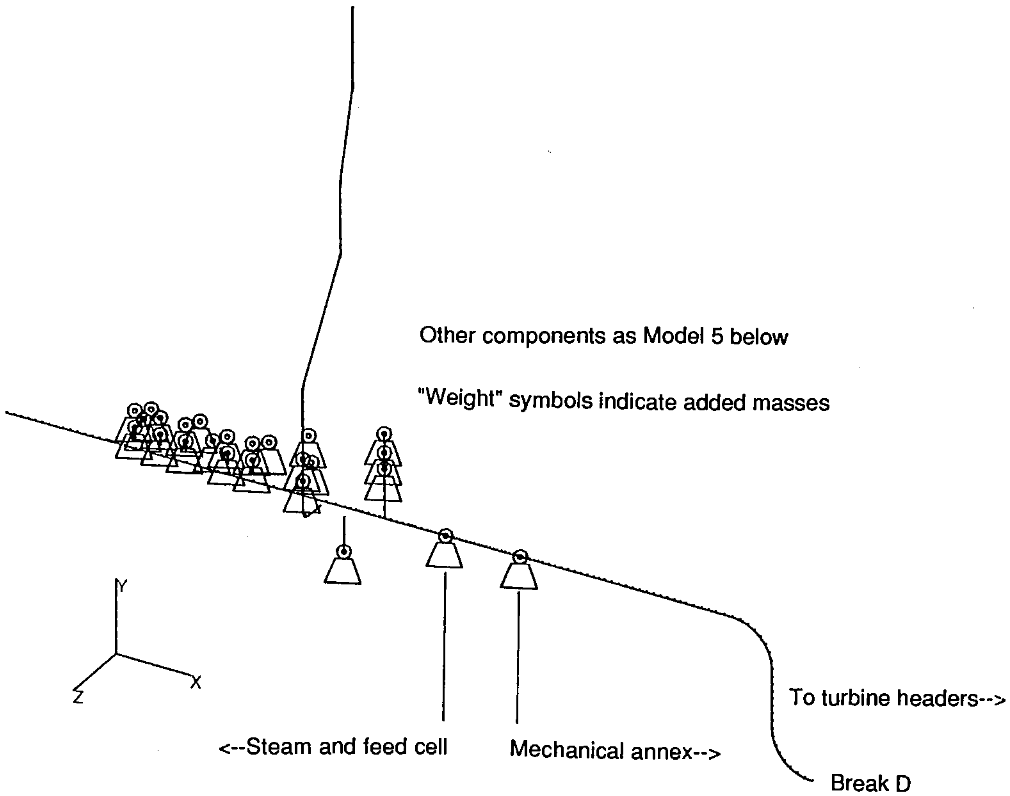

Figure 1: Mathematical model of the main steam line used to analyse break D.

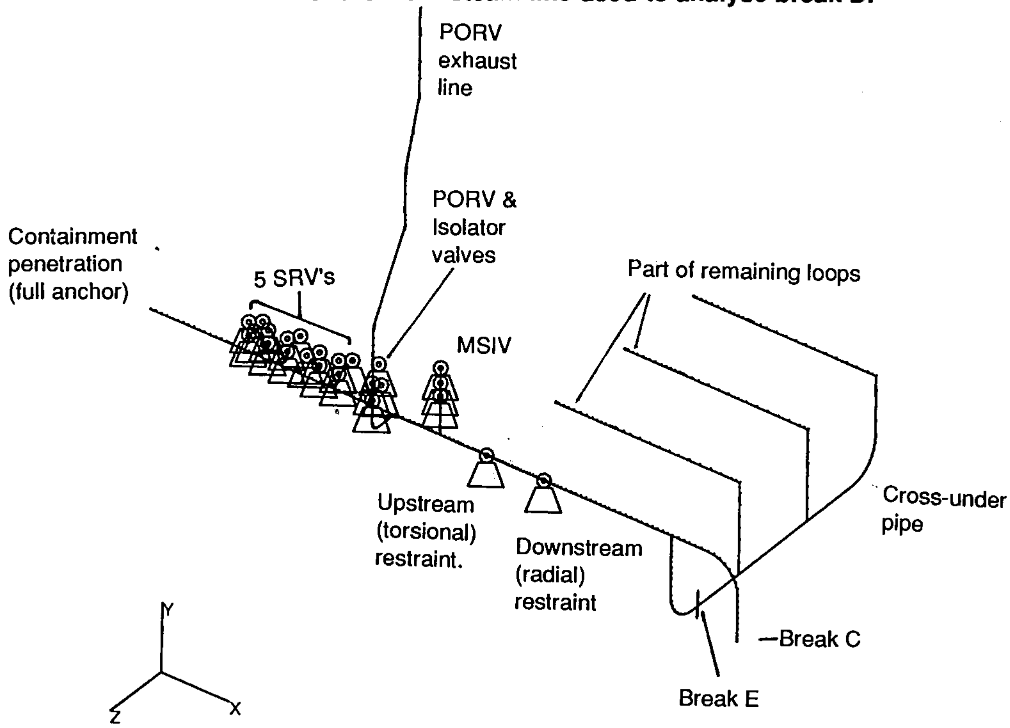

Figure 2: Mathematical model of the main steam line used to analyse break C, with additional mechanical annex pipework.

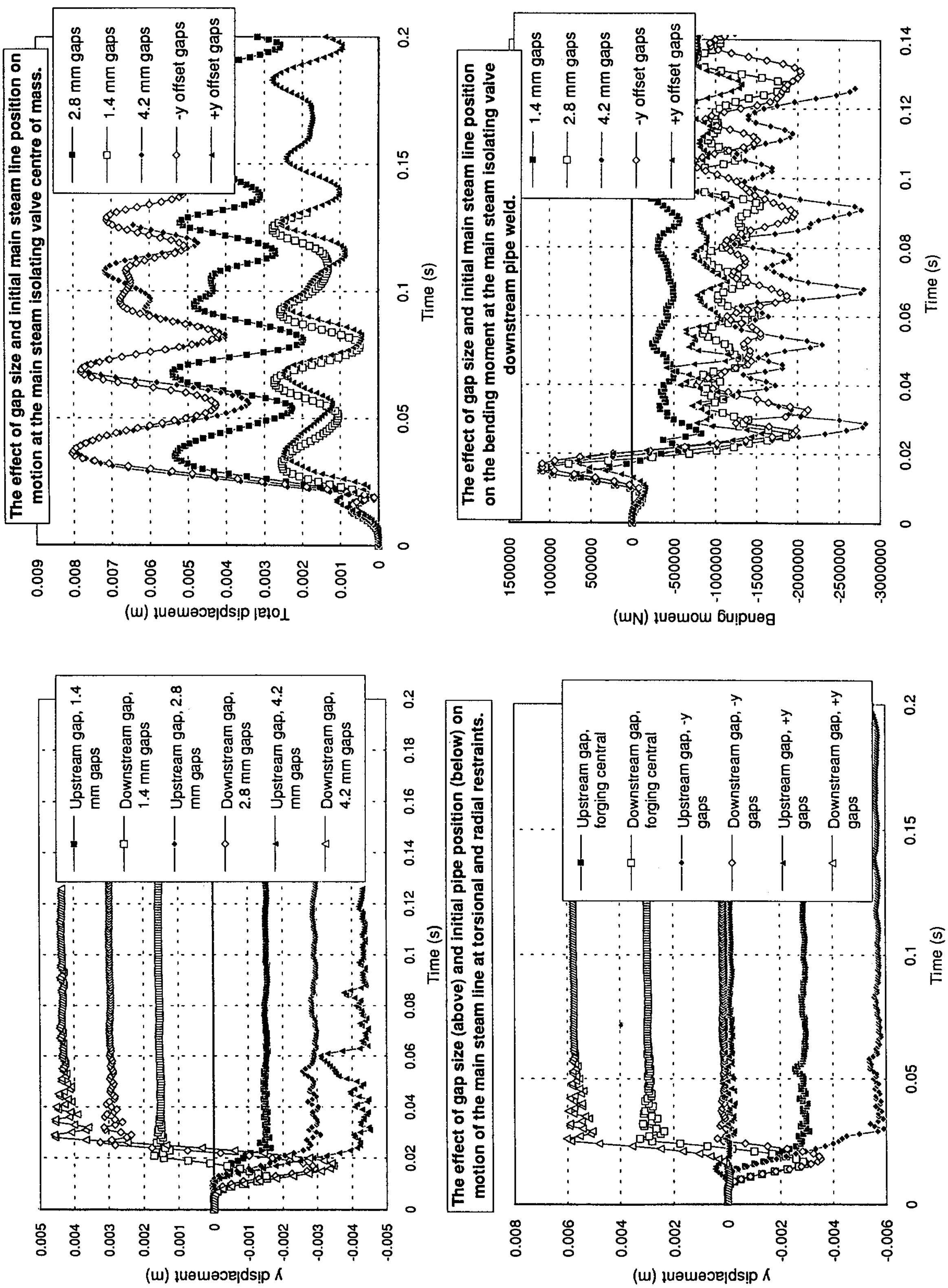

Figure 3: The effect of torsional restraint gap configuration on the response of steam and feed cell components to break C.